

A molecular mechanism for modulating plasma Zn speciation by fatty acids

Jin Lu, Alan J. Stewart, Darrell Sleep, Peter J. Sadler, Teresa J. T. Pinheiro, Claudia A. Blindauer

Supporting Information

E1: Experimental details

Figure S1: Comparison of the zinc binding residues in fatty acid-free and -loaded albumin in 26 published x-ray structures.

Figure S2: ^{111}Cd NMR spectra of rHA with various amounts of octanoate present.

Figure S3: 1D ^1H NMR spectra of the binding of octanoate to recombinant albumin.

Figure S4: ITC data for the addition of Zn^{2+} (333 μM) to BSA (25 μM).

Figure S5: ITC data for the addition of octanoate (333 μM) to BSA (25 μM).

Figure S6: ITC data for the addition of octanoate (20 mM) to BSA (500 μM) in the presence and absence of Zn.

Figure S7: 1D ^1H NMR spectra of the binding of myristate to recombinant albumin.

Figure S8: Example data for ITC data for addition of 333 μM Zn to 25 μM BSA in presence of 3 mol equiv of myristate.

Figure S9: Representative ITC data for the addition of myristate (500 μM) to BSA (12.5 μM)

E1 MATERIALS AND METHODS

Isothermal Titration Calorimetry. BSA was dialyzed against the respective buffer to be used in the titrations (see below) extensively to remove metal ions and fatty acids.¹ A molar absorptivity (ϵ at 280 nm) of 43,824 M⁻¹cm⁻¹,² was used to determine the concentrations of defatted BSA. The Zn²⁺, octanoate and BSA solutions were prepared with the same buffer stock solution, 50 mM Tris buffer with 50 mM NaCl for titrations with Zn²⁺ or octanoate. BSA and myristate solution were prepared in MilliQ water for titrations with myristate. Complexes of BSA with different amounts of Zn²⁺ and fatty acids were prepared by adding carefully measured amounts of the Zn²⁺ or fatty acid to defatted BSA, followed by incubation 2h at 310K.

ITC experiments were performed at 298.0 ± 0.1 K on a Microcal VP-ITC calorimeter (GE Healthcare Science). All samples were degassed by being stirred under vacuum before use. In the cell, the BSA solution had a concentration of 25 μM for titrations with Zn²⁺, and 12.5 μM for titrations with myristate. Octanoate titrations were carried out for BSA concentrations of 25 and 500 μM; the titrant concentrations were adjusted accordingly (see Figures 3, 5 and S4-S6, S8 and S9 for details). In each ITC experiment, 30-35 injections of 6-8 μL of zinc or fatty acids ligand solution were made into the cell containing the sample solution. The first injection was 2 μL, and the data point was discarded, as suggested by Microcal's operation manual. The solution in the cell was stirred at 300 rpm by the syringe to ensure rapid mixing. A background titration, consisting of the identical titrant solution but only the buffer solution in the sample cell, was subtracted from each experimental titration to account for heat of dilution. Data were analyzed with Microcal Origin 7.0, and the fitting curves were calculated according to appropriately selected binding site models. The Origin software uses a nonlinear least-squares algorithm (minimization of χ^2) and the concentrations of the titrant and the sample to fit the heat flow per injection to an equilibrium binding equation, providing best fit values of the stoichiometry (N), change in enthalpy (ΔH), and binding constant (K). In the case of metal complexes, the latter constant is an apparent constant, and can be converted to a stoichiometric constant (which is required to allow meaningful comparisons with literature data) as explained below.

1D ¹H NMR spectroscopy. To eliminate NH resonances, lyophilised samples were dissolved in D₂O (99.9 % isotopic purity, Aldrich) at ca. 50 mg/ml, kept at 295 K for 48 h, and were lyophilised again, and then dissolved

to yield 1 mM solutions in D₂O containing 50 mM NaCl, 50 mM Tris. Sodium formate was added at a concentration of 1 mM as internal calibration standard (8.48 ppm relative to sodium 3-(trimethylsilyl)propionate; TSP). The pH* (pH meter reading) was adjusted to 7.3-7.4; this corresponds to a pD of 7.7-7.8.^[3] 1D ¹H NMR experiments were carried out at 310 K on a Bruker Avance 600 spectrometer operating at 599.82 MHz using a Z-gradient triple-resonance (¹H, ¹³C, ¹⁵N) probe head. Typically, 512 transients were acquired for the 1D spectra (90° excitation pulse, 9 kHz sweepwidth, 8k time domain data points) using a simple presaturation pulse sequence for residual water suppression (1.5 s relaxation delay). The data were zero-filled to 32k, apodised with an optimised combination of squared sine bell and Gaussian functions for resolution enhancement, and Fourier transformed.

Molecular Modelling. The models of myristate and octanoate bound to human serum albumin (Figures 3A and B) were generated within MOE v. 2004.03, using published X-ray structures (1ao6⁴ for ligand-free HSA and 1bj5⁵ for myristate-bound HSA) as starting structures. All energy minimisations described below were carried out after hydrogens had been added. For the model with myristate, the resolved C₁₁ chain present in the FA2 site in pdb 1bj5 was extended by 3 C atoms, and the conformation of the resulting C₁₄ chain, as well as surrounding residues, was optimised by force-field based energy minimisation using a customised version of the AMBER94 force-field. For the HSA model with simultaneously bound octanoate and Zn²⁺, we created a hybrid model by combining pdb structure 1ao6 (ligand-free HSA; residues 5-227 and 292-585), and a fatty-acid containing fragment of domain II encompassing residues 228-291 from pdb 1bj5 (HSA with 5 mol eq of myristate bound), in which octanoate in site FA2 had already been optimised by removing 3 C atoms from the C₁₁ chain, and optimising this pocket via the procedure described above for myristate. The hybrid model then was further processed by adding a Zn²⁺ ion. The Zn site was energy minimised using a step-wise procedure (Zn, bound atoms, residues, surroundings). The octanoate site in the hybrid model was subsequently optimised again in its new surroundings. Finally, the entire molecule was subjected to force-field based energy minimisation to mend bad geometries introduced by the combination of the three fragments. Resulting structures were validated using the WHATIF web interface,⁶ ensuring that physically reasonable models had been obtained.

Conversion from apparent to stoichiometric constants

Note that the following corrections are based on the assumption that ternary complexes between BSA, Tris and Zn^{2+} do not play a significant role in the equilibria.

For a 1:1 complex of Zn (M) with albumin (A), the association constant is given by

$$K_{MA} = \frac{[MA]}{[M][A]}$$

Constants captured by ITC are an apparent constants, meaning that they are based on total metal and albumin concentrations; $[M]_{total}$ and $[A]_{total}$ refer to the portion of M and A that are NOT part of the complex MA:

$$K_{app(M-A)} = \frac{[MA]}{[M]_{total}[A]_{total}}$$

The actual metal concentration is affected by metal-buffer (T, for Tris) interactions, and the actual binding site concentration is affected by the protonation equilibrium for the binding site:

$$K_{app(M-A)} = \frac{[MA]}{([M] + [MT])([A] + [HA])}$$

$[MT]$ and $[HA]$ can be estimated using the apparent Zn(Tris) binding constant ($K_{app(M-T)}$) and the pK_a value for the protonation of the binding site on albumin, respectively:

$$K_{app(M-A)} = \frac{[MA]}{([M] + K_{app(M-T)} \times [M] \times [T])([A] + \frac{[H^+] \times [A]}{K_a})}$$

$$= \frac{[MA]}{[M] \times [A] \times (1 + K_{app(M-T)} \times [T]) \left(1 + \frac{[H^+]}{K_a}\right)}$$

$$= K \times \frac{1}{(1 + K_{app(M-T)} \times [T]) \times \left(1 + \frac{[H^+]}{K_a}\right)}$$

$$K_{app(M-A)} = K \times \frac{K_a}{(1 + K_{app(M-T)} \times [T]) \times (K_a + [H^+])}$$

$$K = K_{app(M-A)} \times \frac{(1 + K_{app(M-T)}[T]) \times (K_a + [H^+])}{K_a} \quad (1)$$

In the present study, 50 mM Tris-buffered solutions at pH 7.2 were employed. The binding constant for the Zn(Tris) complex is also pH dependent. With $\log K_{Zn-T} = 2.271^7$ and $pK_a(\text{Tris}) = 8.11^7$, the apparent binding constant for the Zn(Tris) complex can be calculated:

$$\begin{aligned} \log K_{app(Zn-T)} &= \log K_{Zn-T} + \log K_a - \log(K_a + [H^+]) \\ &= 2.271 - 8.11 - \log(10^{-8.11} + 10^{-7.2}) \\ &= 2.271 - 8.11 + 7.150 \\ &= 1.311 \end{aligned}$$

Since the reduction in total Tris concentration due to its interactions with Zn is very small compared to the total concentration, [T] can be approximated by the total concentration.

Hence, with $K_{app(Zn-BSA)} = 10^{5.67}$ at a pH = 7.2 from the ITC experiment, a literature value for $pK_a(\text{BSA}) = 8.2^8$ and $\log K_{app(Zn-T)} = 1.311$. Eq (1) becomes:

$$K_{Zn-BSA} = 10^{5.67} \times \frac{(1 + 10^{1.3} \times 0.0) \times (10^{-8.2} + 10^{-7.2})}{10^{-8.2}}$$

And hence, for the first stoichiometric binding constant of Zn^{2+} and BSA: **$\log K_{Zn-BSA} = 7.02$**

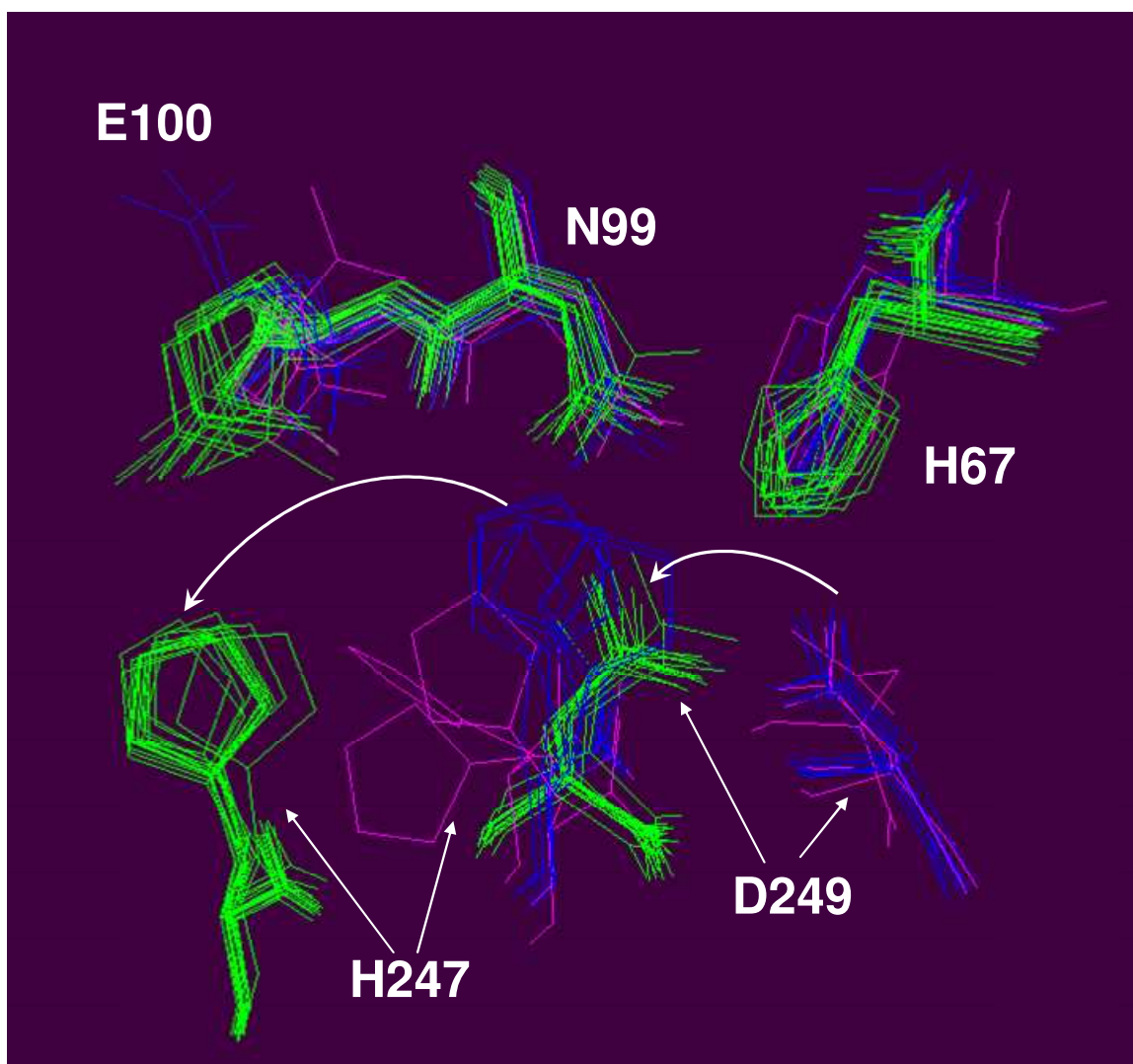


Figure S1: Comparison of the zinc binding site in fatty acid-free (blue) and -loaded (green) albumin in 26 available x-ray structures. The overlays were generated and are displayed in Swiss pdb viewer v 3.7, by first fitting all atoms of residues His67 and Asn99, and then generating an improved fit. The structures in purple are those (1uor, 1hk2, 1tf0), in which the side-chain conformation of His247 differs considerably from that observed in other fatty-acid-free structures. Albumin in 1tf0 has three molecules of decanoate bound, but none in site FA2. The white bent arrows indicate the movement of the domain-II residues His247 and Asp249 relative to the domain-I half of the binding site. E100 forms an H-bond with His247 in fatty-acid loaded albumin.

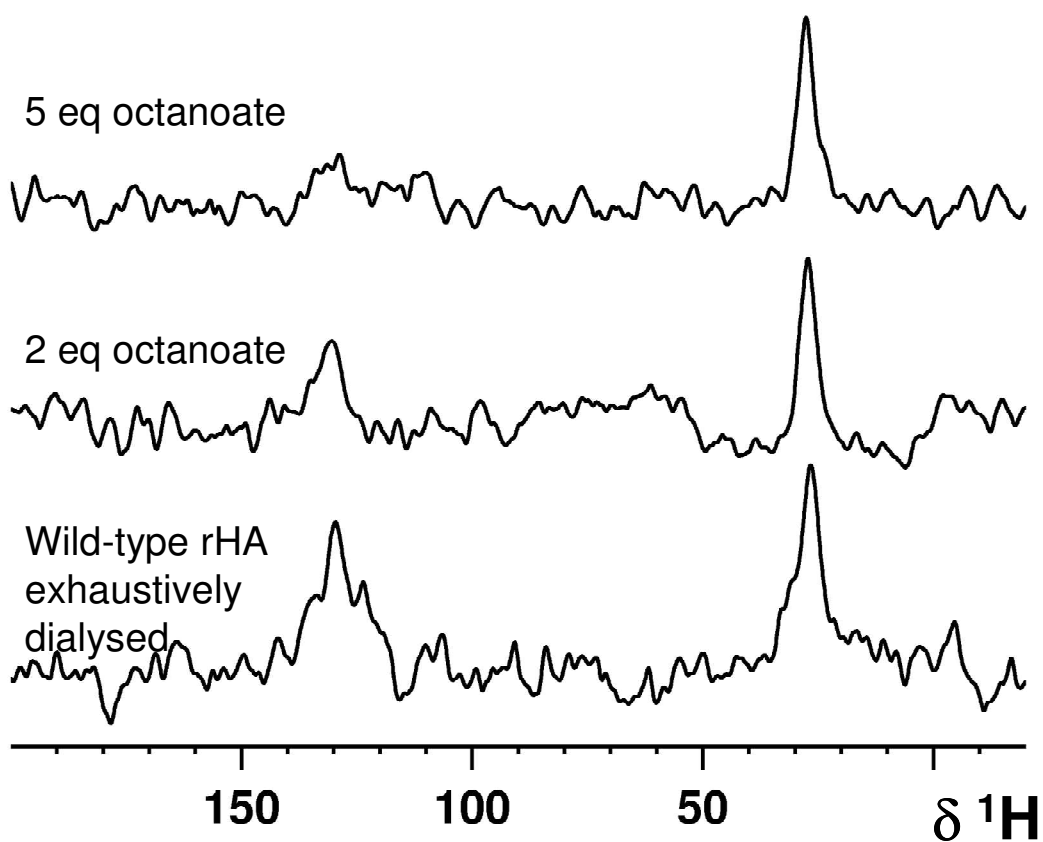


Figure S2: ^{111}Cd NMR spectra of recombinant human serum albumin with various amounts of octanoate present. The low-field peak corresponds to the high-affinity zinc site.^{1,7} Cd^{2+} binding to this site is clearly perturbed by the presence of octanoate. The absence of a peak does not necessarily mean that Cd^{2+} cannot bind, but can also be caused by changes in the exchange dynamics.

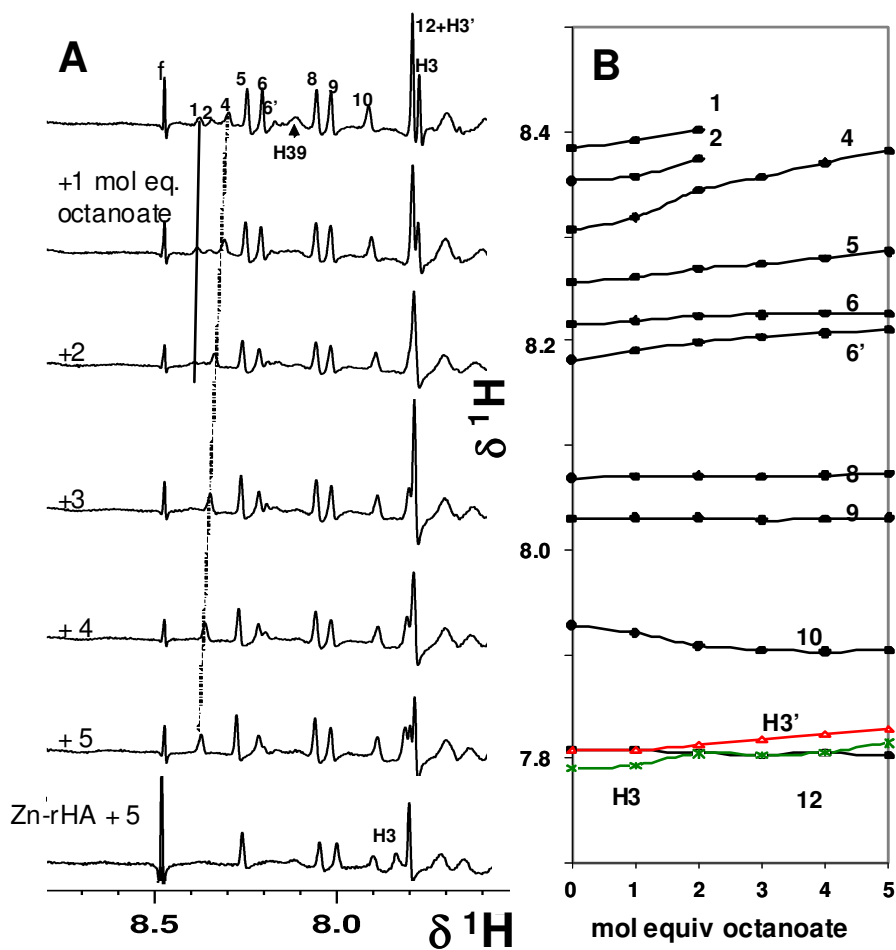


Figure S3: 1D ^1H NMR spectra monitoring the binding of octanoate to recombinant albumin. Solutions of albumin (1 mM) were prepared in 50 mM $[\text{D}_{11}]\text{Tris-Cl}$, 50 mM NaCl, 100% D_2O (v/v), $\text{pH}^* 7.4$, 310K. $\text{H}\epsilon 1$ proton resonances are labeled with numbers from 1 to 12. f denotes formate, added as a chemical shift reference. Peak 1 and 4 are assigned to His67 and His247.

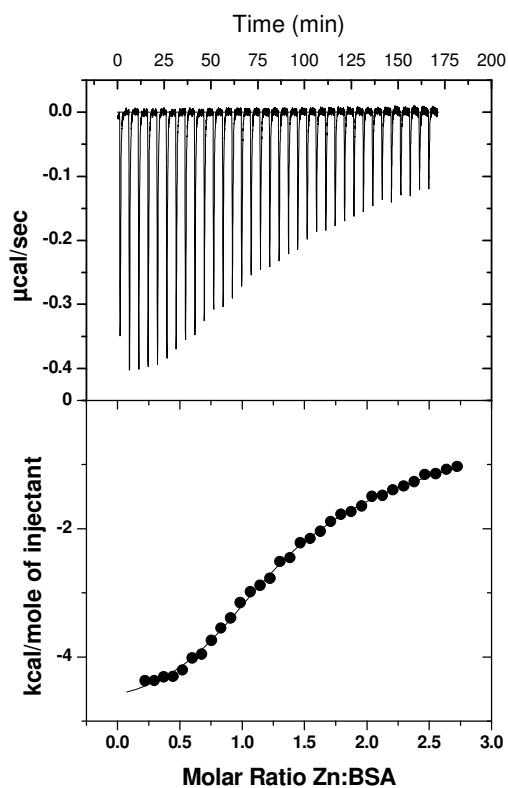


Figure S4: ITC data for the addition of Zn^{2+} (333 μM) to BSA (25 μM) in 50 mM Tris-Cl buffer with 50 mM NaCl, pH 7.2. The upper panel shows the calorimetric titrations with 8 μL injections with 240 s time between injections to allow complete equilibration. 34 injections had been added. Blank titrations of 50 mM Tris-Cl, pH 7.2, with Zn^{2+} (333 μM) were performed and the dilution heats were subtracted. The lower panel represents the background-subtracted, integrated heat values as a function of the Zn^{2+} -to-BSA molar ratio in the cell. The solid line corresponds to a fit to a model with 2 sequential binding sites ($\log K_1 = 5.68$, $\log K_2 = 4.27$).

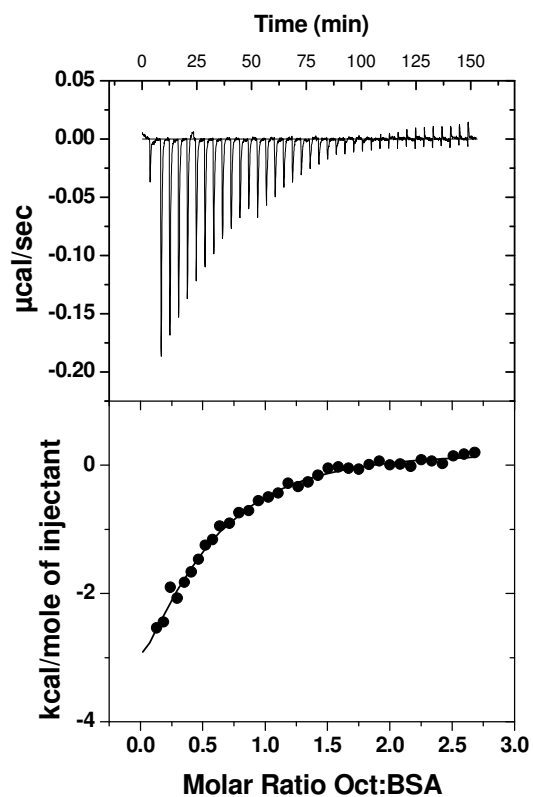


Figure S5: ITC data for the addition of octanoate (333 μM) to BSA (25 μM). 34 injections of 8 μl of 333 μM octanoate were delivered with an adequate interval (240 s) between injections to allow complete equilibration. Blank titrations of 50 mM Tris-HCl, pH 7.2, with octanoate (333 μM) were performed and the dilution heats were subtracted. The lower panel represents the background-subtracted, integrated heat values as a function of the Octanoate-to-BSA molar ratio in the cell. The solid line represents a fit for two sets of binding sites with $\log K_1 = 5.0$ and $\log K_2$ set to 3.3. The latter value was derived from titrations at higher concentrations (Figure 3B and S6).

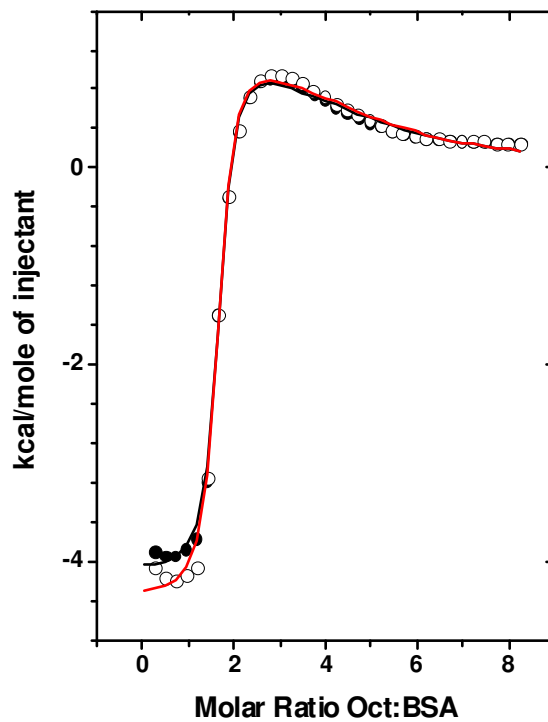


Figure S6: ITC data for the addition of octanoate (20 mM) to BSA (500 μ M) in the presence (filled circles, black line) and absence (empty circles, red line) of 1 molar equivalent of Zn^{2+} . The fits correspond to models with 2 sets of binding sites; $\log K_1 = 5.64$, $N = 1.54$ and $\log K_2 = 3.30$; $N = 3.21$ (red fit). $\log K_1 = 5.62$, $N = 1.56$ and $\log K_2 = 3.24$; $N = 3.13$ (black fit).

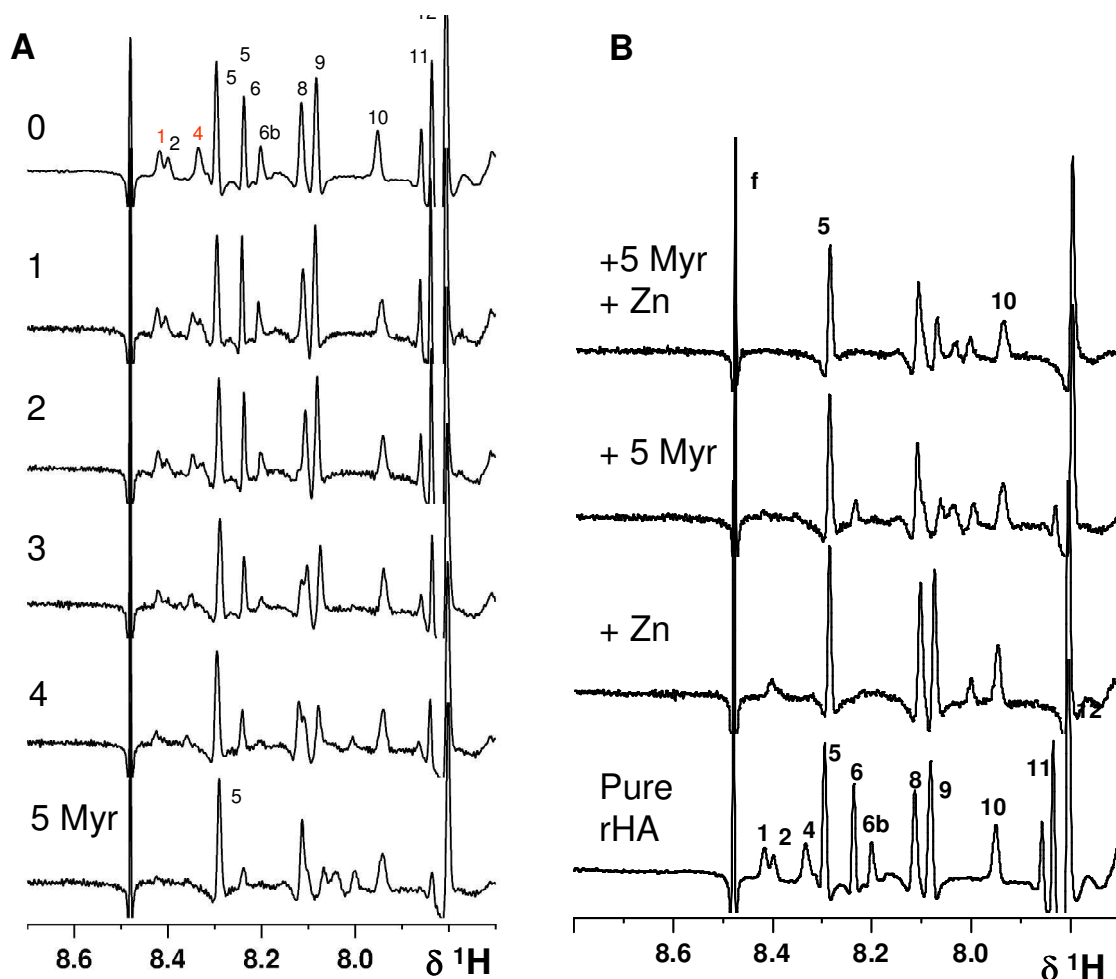


Figure S7: 1D ¹H NMR spectra monitoring the binding of myristate to recombinant human serum albumin in the presence and absence of zinc. Solutions of albumin (1 mM) were prepared in 50 mM [D₁₁]Tris-Cl, 50 mM NaCl, 100% D₂O (v/v), pH* 7.2, 318K. He1 proton resonances are labeled with numbers from 1 to 12. “f” denotes formate, added as a chemical shift reference. (A) Titration with myristate in the absence of zinc. (B) Comparison of ¹H NMR spectra of rHA in the presence of zinc and myristate. Peaks 1 and 4 are assigned to His67 and His247, part of the high-affinity zinc site A. Addition of myristate leads to the disappearance of both these peaks, consistent with the notion that long-chain fatty acid binding to site FA2 rigidifies the domain/II interface. The effects of octanoate binding are significantly different (Figure S3), since peak 4 sharpens rather than broadens. This suggests a different binding mode for octanoate, as illustrated in Figure 4B.

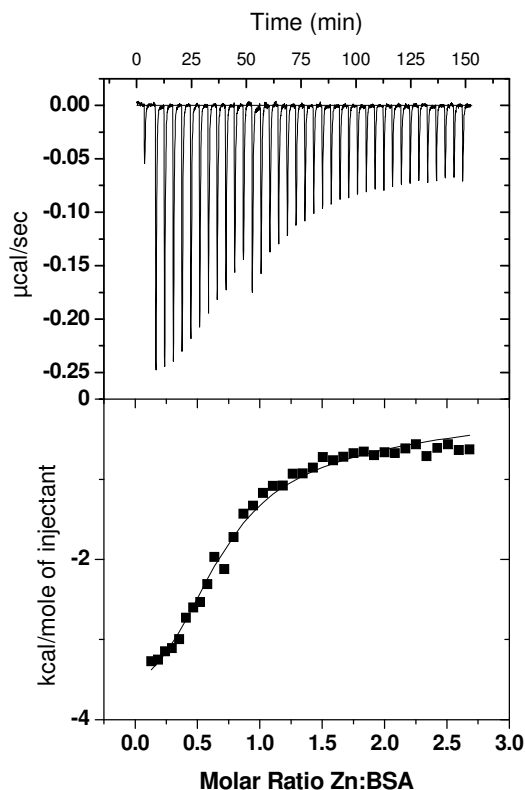


Figure S8. Example data for isothermal titration calorimetry data for addition of 333 μM Zn to 25 μM BSA in presence of 3 mol equiv of myristate. The fit corresponds to a model with two sets of sites, and the purpose of the fits was to determine the stoichiometry for site A. The underlying hypothesis behind the choice of this model is that fatty acids completely block zinc binding site A. Generally, the information content of the data is insufficient to allow all six parameters to vary in this model; hence $\log K_1 = 5.67$ and $\log K_2 = 4.15$, the values determined in titrations in the absence of myristate (Figure S4), were held constant. N_2 was set to 1, and ΔH_1 and ΔH_2 as well as N_1 were allowed to vary. The result for N_1 in this case was 0.60 ± 0.03 . Alternative fits are possible; if N_2 is allowed to vary, but ΔH_1 and ΔH_2 are held constant at -5193 and -8740 kJmol^{-1} (values derived from titrations in the absence of Myr, fitted with two sequential sites, Figure S4), $N_1 = 0.34$ is obtained. If both N and ΔH values are varied, $N_1 = 0.61$; however N_2 moved to 3.86 ± 2.51 . In each case, the data plotted in Figure 4B take into account all three of these fitting attempts. The datasets with 0-3 mol equiv of myristate were treated as described above, the dataset for 4 and 5 mol equiv of myristate were fitted with both K and ΔH fixed and both N were allowed to vary. In the latter cases, N_2 values were 0.22 and 0.15.

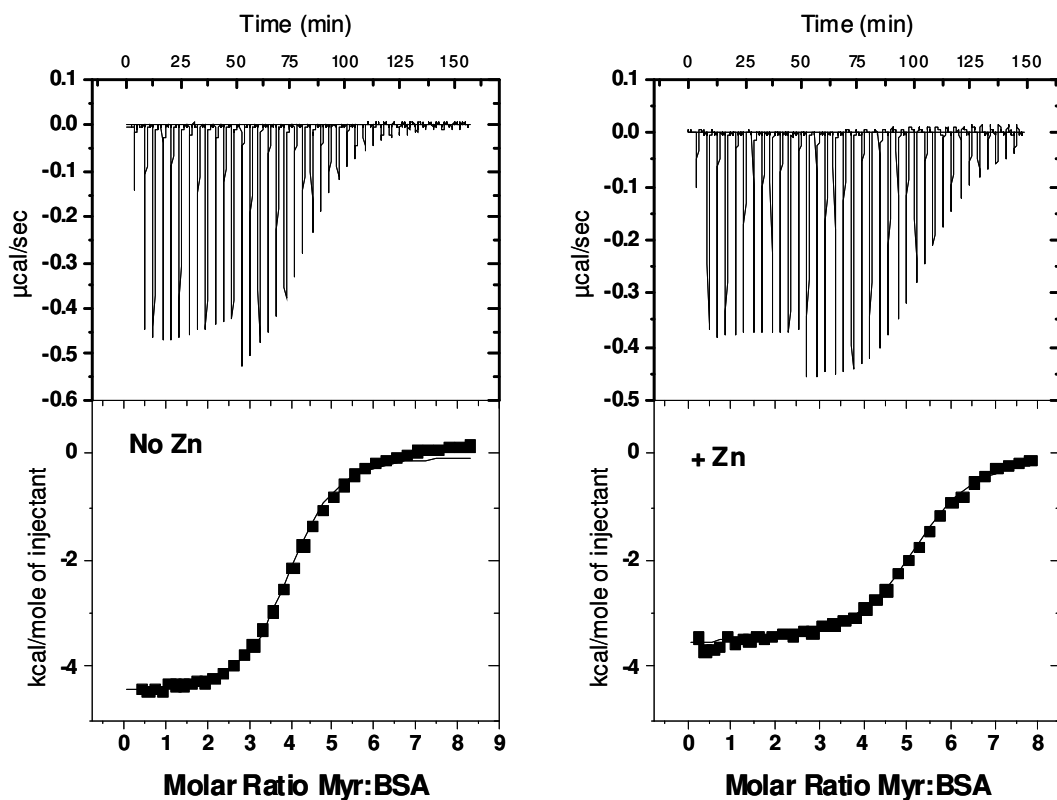


Figure S9: Representative ITC data for the additions of myristate (500 μM) to BSA (12.5 μM , H_2O , pH 7.8). After a first injection of 2 μl , 11 injections of 6 μl and 24 injections of 8 μl of a 500 μM myristate solution in H_2O (pH 7.8) were delivered with an adequate interval (240 s) between injections to allow complete equilibration. The lower panel represents the integrated heat values as a function of the myristate-to-BSA molar ratio in the cell. The solid lines represent fits for one set of binding sites with $\log K = 6.1$ (without Zn) or 5.95 (with Zn).

References

- (1) Stewart, A. J.; Blindauer, C. A.; Berezenko, S.; Sleep, D.; Sadler, P. J. *Proc. Natl. Acad. Sci. U.S.A.* **2003**, *100*, 3701-3706.
 - (2) Peters, T.; in *The Plasma Proteins*. (Putman F. W., ed.), Academic Press 1975, 133–181.
 - (3) Glasoe, P. K. and Long, F. A. *J. Phys. Chem.* **1960**, *64*, 188-189.
 - (4) Sugio, S.; Kashima, A.; Mochizuki, S.; Noda, M.; Kobayashi, K. *Protein Eng.* **1999**, *12*, 439-446.
 - (5) Curry, S.; Mandelkow, H.; Brick, P.; Franks, N. *Nat. Struct. Biol.* **1998**, *5*, 827-835.
 - (6) <http://swift.cmbi.ru.nl/servers/html/index.html>
 - (7) Bologni, L.; Sabatini, A.; Vacca, A. *Inorg.Chim. Acta.* **1983**, *69*, 71-75
 - (8) Ohyoshi, E.; Hamada, Y.; Nakata, K.; Kohata, S. *J. Inorg. Biochem.* **1999**, *75*, 213-218.
- Full reference 4(b):** Costarelli, L.; Muti, E.; Malavolta, M.; Cipriano, C.; Giacconi, R.; Tesei, S.; Piacenza, F.; Pierpaoli, S.; Gasparini, N.; Faloia, E.; Tirabassi, G.; Boscaro, M.; Polito, A.; Mauro, B.; Maiani, F.; Raguzzini, A.; Marcellini, F.; Giuli, C.; Papa, R.; Emanuelli, M.; Lattanzio, F.; Mocchegiani, E. *J. Nutr. Biochem.* **2010**, *21*, 432-437.